ELSEVIER

Journal of Nuclear Materials 307–311 (2002) 1146–1151

journal of nuclear materials

www.elsevier.com/locate/jnucmat

Conductivity of SiC during neutron and proton irradiation

O.A. Plaksin [a,*], V.A. Stepanov [a], H. Amekura [b], N. Kishimoto [b]

[a] *SSCRF – A.I. Leypunsky Institute of Physics and Power Engineering, Obninsk, Kaluga Region 249033, Russia*
[b] *Nanomaterials Laboratory, National Institute for Materials Science, Sakura, Tsukuba, Ibaraki 305-0003, Japan*

Abstract

The radiation-induced conductivity (RIC) of single crystalline 6H-SiC has been measured in a pulsed fission reactor (BARS-6: the pulse-width is 80 μs, dose rate $<1.5 \times 10^5$ Gy/s) and under 17 MeV proton irradiation (dose rate $<5 \times 10^3$ Gy/s). The magnitude of RIC has been compared by normalizing the ionizing dose rates. The RIC efficiency of the pulsed reactor irradiation is four times lower than the proton irradiation. To explain the lower RIC efficiency, we point out importance of cascade effects induced by pulsed neutrons, though the RIC consists of synergistic processes. Spatial distribution of energy loss of pulsed neutrons is more irregular than that of protons, due to the different distribution and parameters of cascades. The carrier production rate is not constant in the microscopic region of the material but abruptly changes by several orders of magnitude. During the reactor irradiation, intense charge carrier production (at least 10^3 times faster) occurs in the microscopic regions (size up to ~1000 nm) occupying a small part (lower than 10^{-3}) of the bulk SiC. The localized ionization is due to dense tracks of primary recoil ions and atomic collision cascades. Sharp spikes of charge carrier production may considerably contribute to the mean carrier-production rate, but, due to non-additive contributions, their effect on overall conductivity is not dominant.

1. Introduction

Studying mechanisms of radiation-induced processes in SiC-based materials is one of the key issues for prospective application in thermonuclear reactors, such as first-wall components and radiation–resistant electronic devices [1]. Since SiC-based materials are more radiation–resistant than other semiconductors, radiation-induced processes under various particle irradiation can be reliably compared with each other.

Measurements of radiation-induced conductivity (RIC) enable one to determine the kinetic parameters of the electric charge transport (mobility, electron–hole recombination coefficient, trapping coefficients, etc.) and assess effects of ionization on the properties of the materials under irradiation of various types. The contribution of ionization to electrical conductivity depends on the irradiation conditions. One of the important factors determining the contribution of ionization to electrical conductivity is the degree of inhomogeneity of ionization in the solid. Moreover, when the radiation energy is deposited in microscopic regions, the electron–hole recombination may result in the local energy release and occasionally in transformation of the structure. In the present study, the RIC of single crystalline SiC during pulsed reactor irradiation has been measured. The data on RIC during reactor irradiation are compared to those for proton irradiation and the different contributions of ionization to electrical conductivity of SiC are discussed.

2. Electrical properties of SiC

Complex structure and phases of SiC composites make it difficult to study radiation-induced processes therein. There are more than 140 polytypes known with different arrangement of cubic and hexagonal planes in the close-packed structure of SiC. The electrical

* Corresponding author. Tel.: +7-08439 98382; fax: +7-95 230 2326.
E-mail address: plax@mail.ru (O.A. Plaksin).

0022-3115/02/$ - see front matter
PII: S0022-3115(02)00953-4

Table 1
Electrical properties of the polytypes of SiC [2]

Polytype	4H-SiC	6H-SiC	3C-SiC
Band gap, eV	3.2	3.0	2.3
Electric break-down strength, MV/cm	2–3	2–3	>1.5
Electron mobility (300 K), cm^2/V s	800	200–300	1000
Hole mobility (300 K), cm^2/V s	60	50	40

characteristics of typical polytypes of SiC are presented in Table 1.

The electrical properties of SiC also depend on the impurity and intrinsic defect concentration. Since the ionization energies of acceptors and donors in SiC (both impurities and intrinsic defects) usually exceed 0.1 eV, these defects are regarded as deep traps [2]. Different impurities and intrinsic defects affect the stability of different polytypes [2].

The electrical processes in dielectrics and semiconductors under irradiation depend on the rates of free charge carrier production $G(t)$, electron–hole recombination and charge carrier trapping in the intrinsic defects and impurities. Evolution of free charge carriers during excitation (irradiation) of semiconductors is usually given by the generalized Shockley-Read equations [3]. To consider the kinetics of charge carrier recombination and trapping kinetics separately, a somewhat modified approach is more convenient [4]. For example, assuming a single type of donors and a single type of acceptors, the evolution of free and trapped charge carriers is given by the following equations

$$\dot{p} = G(t) - w_{\text{e–h}} np - w_{\text{h-A}}(c_{\text{A}} - c_{\text{h}})p - w_{\text{h-D}} c_{\text{e}} p + w_{\text{h}} c_{\text{h}}, \tag{1}$$

$$\dot{n} = G(t) - w_{\text{e–h}} np - w_{\text{e-D}}(c_{\text{D}} - c_{\text{e}})n - w_{\text{e-A}} c_{\text{h}} n + w_{\text{e}} c_{\text{e}}, \tag{2}$$

$$\dot{c}_{\text{h}} = w_{\text{h-A}}(c_{\text{A}} - c_{\text{h}})p - w_{\text{h-D}} c_{\text{e}} p - w_{\text{h}} c_{\text{h}}, \tag{3}$$

$$\dot{c}_{\text{e}} = w_{\text{e-A}}(c_{\text{D}} - c_{\text{e}})n - w_{\text{e-D}} c_{\text{h}} n - w_{\text{e}} c_{\text{e}}, \tag{4}$$

where p and n are free hole and electron densities, c_{A} and c_{D} are acceptor and donor concentrations, c_{h} and c_{e} are trapped hole and electron densities, $w_{\text{e–h}}$ is a coefficient of electron–hole recombination, $w_{\text{h-A}}$, $w_{\text{h-D}}$, $w_{\text{e-A}}$ and $w_{\text{e-D}}$ are trapping coefficients for holes (h) and electrons (e) at acceptors (A) and donors (D), w_{h} and w_{e} are probabilities of the hole and electron escape from acceptors and donors, respectively. In the both approaches mentioned the material and irradiation field are considered to be uniform. The formulation enables one to describe the conductivity of single crystals, glasses and ceramics under electron, proton and roentgen irradiation, the RIC well corresponding to the ionizing dose rates [4]. Nevertheless, non-uniformity may be essential for RIC. For example, microscopically non-uniform ionization (due to dense tracks or cascades) may result in RIC different from the RIC during uniform irradiation. In general, it is rather difficult to consider non-uniformity in these approaches. However, the Eqs. (1)–(4) may be used to assess non-uniformity qualitatively when calculated parameters differ from those calculated for uniform conditions.

There are few studies on the electrical properties of SiC under neutron irradiation [5,6]. The temperature dependence of the electrical conductivity of polycrystalline SiC before and after gamma irradiation (activation energy 1.1 eV) and also electron and neutron irradiation (activation energy 1.4 eV) were explained by the ionic conductance [5,6]. However, those dependencies and radiation-induced changes of the conductivity may be explained by the electric charge transport via deep traps, whose concentration in polycrystalline SiC is high due to high concentrations of the intrinsic defects and impurities.

For example, during gamma irradiation (dose rate 38 Gy/s, dose 4.2×10^4 Gy) of hot-pressed and reaction-sintered polycrystalline SiC at temperatures from 723 to 873 K, a slow increase of the conductivity (total ~20%), its saturation at the dose of 2.5×10^4 Gy and its recovery in subsequent annealing for 1 h at the same temperature were observed. Instantaneous contribution of RIC were not observed. It was probably difficult due to the low density of radiation-induced charge carriers, which resulted from the high concentration of deep traps in polycrystalline SiC. Taking into account the observed conductivity ($\sim 5 \times 10^{-5}$ S/cm) and the trap levels (1.1 eV) and the temperature, the trap concentration in polycrystalline SiC could be about 10^{20}–10^{21} cm^{-3}. The increase of the conductivity during irradiation may be related to the filling of the deep traps and, hence, the increase of hopping mobility. The concentration N_{tf} of traps, that may be filled during gamma irradiation, may be evaluated with the following expression [7]

$$N_{\text{tf}} = \frac{\rho \dot{D} \tau}{E_{\text{e–h}}}, \tag{5}$$

where $\dot{D}$ is the dose rate (38 Gy/s), ρ is the density of the material (~3 g/cm^3), $E_{\text{e–h}}$ the energy of electron–hole pair formation (~2–2.5 E_{g}), E_{g} is a band gap (~3 eV). If the characteristic time of the RIC increasing ($\sim 10^3$ c) is assumed to be equal to the characteristic time of the trap filling τ, then N_{tf} is about 10^{20}–10^{21} cm^{-3}.

Determination of electrical characteristics may be important not only in the engineering aspect but also for understanding the difference between neutron and other particle irradiation. Characteristics of charge carrier

recombination and trapping (trapping cross-sections (σ_p, σ_n) or trapping coefficients) in SiC polytypes are unknown, to a great extent. Moreover, the trapping cross-sections may vary in a wide range, as for Al impurities ($\sigma_p = 3.6 \times 10^{-12}$ and 1.3×10^{-15} cm^2 for two acceptor levels, $\sigma_n \sim 10^{-22}$ cm^2 for the donor level). The characteristics of charge carrier trapping and recombination for various structures of SiC and impurity contents therein may be calculated from the data on RIC obtained during pulsed irradiation. In the present study a pulsed reactor irradiation of undoped single crystalline SiC have been conducted, since the low impurity content in these crystals enables one to determine both the trapping and recombination characteristics.

Then, the determined characteristics were used for calculation of steady-state RIC under reactor irradiation. This enables us to compare our results with the steady-state RIC measured during proton irradiation, with the purpose to assess the ionizing efficiency of neutrons and obtain understanding of the processes involving charge carriers during conversion of the energy deposited by neutrons.

3. Experimental

Measurements of RIC of single crystalline 6H-SiC (initial conductivity 1.3×10^{-3} S/cm) were conducted on the BARS-6 pulsed fast fission reactor (IPPE, pulse duration 80 μs, dose per pulse $<5.5 \times 10^{12}$ n/cm^2 (12 Gy), dose rate $<7 \times 10^{16}$ n/cm^{2}s (1.5×10^5 Gy/s)). The specimens with a boron and nitrogen content of about 10^{17} cm^{-3} were produced using a bulk sublimation method [8]. Before irradiation specimens show p-type conductivity with a hole concentration of 1.6×10^{14} cm^{-3}. Temperature dependence is compatible with an activation energy of ~0.3 eV (acceptor levels of boron). Ohmic electrodes were made by vacuum evaporation of Al and subsequent annealing in argon at 1173 K for 30 min.

For measurements, we used a planer electrode technique and a measuring system based on multichannel ADC (resolution time >100 ns) and PC. The neutron pulse was registered by means of an evacuated fission chamber placed in a boron-containing case (for counting neutrons with an energy >0.5 eV). The dose per pulse was determined from the residual activity of nickel samples. The absorbed dose was calculated with the aid of the MCNP code [9] taking into account the energy transfer due to gamma irradiation, the collisions involving neutrons and neutron absorption. According MCNP code calculation their contributions to the total absorbed dose are equal to 20–25%, 55–65% and 15–20%, respectively.

Steady-state RIC was measured during proton irradiation (NIMS cyclotron, proton energy 17 MeV, dose rate $<1 \times 10^{12}$ p/cm^{2}s (5×10^3 Gy/s)). The sample was attached to a temperature-stabilized holder, and the temperature was kept at 300 ± 1 K. Results on conductivity measurements during proton irradiation have been presented in more details elsewhere [8].

4. Results

A typical time dependence of RIC of 6H-SiC during a reactor pulse is given in Fig. 1. It is seen, that RIC has a fast and a slow component. The fast component obeys a power law depending on the neutron flux (or dose rate) with an exponent of 0.69. After the fast component, more than 100 μs after the maximum of the RIC, the slow component is observed as a tail with a characteristic decay time of about 1 ms.

To analyze the time dependence of the RIC of 6H-SiC single crystal, the system of Eqs. (2)–(5) was numerically solved. The electrical conductivity was calculated from the expressions

$$\sigma = e\mu_h f(t), \tag{6}$$

$$\text{with} \quad f(t) = p(t) + \frac{\mu_e}{\mu_h} n(t), \tag{7}$$

where e was an elementary charge. The mobilities of free electrons (μ_h) and holes (μ_e) were taken as constants in the calculation. The ratio of the electron mobility to the hole mobility was taken equal to 5 (see Table 1). It was assumed that boron and nitrogen were the main acceptor and donor impurities, respectively. Partial compensation of boron by nitrogen was also considered. The

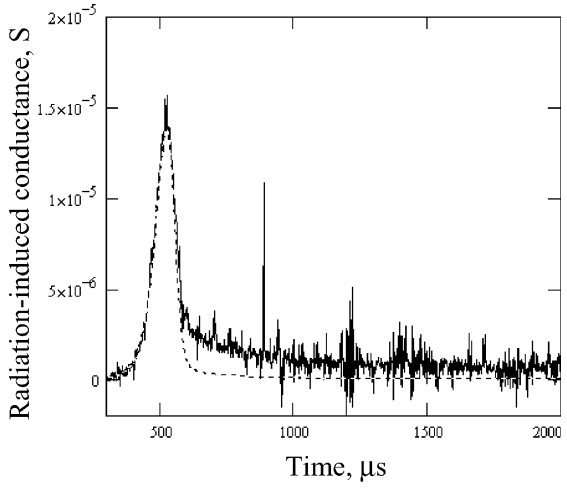

Fig. 1. Time dependence of radiation-induced conductance of 6H-SiC during a pulse of the reactor. Dashed line corresponds to the neutron flux in the power of 0.69 (given in arbitrary units).

temperature dependence of the initial conductivity indicates that the difference in boron and nitrogen concentrations was much higher than the initial free hole density $p(0)$ in 6H-SiC. To avoid uncertainty in calculations, c_A and c_D were put equal to 1.6×10^{17} and 1.2×10^{17} cm^{-3}, respectively. Accounting partial compensation, the initial density of trapped holes $c_h(0)$ was equal to $c_B - c_N - p(0)$, and the initial density of trapped electrons $c_n(0)$ was equal to zero.

The rate of electron–hole pair production $G(t)$ was calculated from the ionizing dose rate $\dot{D}(t)$ according to

$$G(t) = \frac{\rho \dot{D}(t)}{E_{e\text{–}h}}, \tag{8}$$

where ρ is a density of 6H-SiC (3.21 g/cm^3). In the Table 2, the coefficients of recombination, trapping and detrapping calculated are given for the cases when the ionizing dose rate was taken equal to (a) the total absorbed dose and (b) the dose absorbed due to collisions involving neutrons and gamma radiation (80% of total absorbed dose). Fig. 2 represents the time dependence $f(t)$ and time dependencies of charge carrier densities calculated for the case (a).

The determination of the parameters of the system of Eqs. (2)–(5) by its numerical solution is rather reliable. In particular, assuming constant carrier mobilities, the observed sub-linear dose rate dependence of RIC and the slow component of RIC indicate the rates of electron–hole recombination, charge carrier trapping and electron–hole pair production being of the same order of magnitude. It limits the range of values of the coefficients of recombination (10^{-8}–10^{-7} cm^3/s) and trapping. For comparison, calculations were done (Table 2) using data presented in Ref. [8] on the steady-state RIC of similar specimens of 6H-SiC under continuous proton irradiation with an energy of 17 MeV and a dose rate $<5 \times 10^3$ Gy/s at 300 K. In Ref. [8] a sub-linear (power 0.77) dose rate dependence of steady-state RIC was also reported, and it was explained by electron–hole recombination prevailing. The sub-linear dose rate dependence of the steady-state RIC during continuous proton irradiation indicates that the sub-linear dependence of the RIC during pulsed reactor irradiation is due to electron–hole recombination prevailing, not charge carrier release from traps.

Table 2
Kinetic parameters of charge carrier recombination, trapping and detrapping

Parameter	(a) Total absorbed dose	(b) 80% of total absorbed dose	Proton irradiation
$w_{e\text{–}h}$, cm^3/s	7.3×10^{-8}	5.2×10^{-8}	2.4×10^{-8}
$w_{e\text{-}D}$, cm^3/s	1.7×10^{-10}	1.5×10^{-10}	2.6×10^{-10}
$w_{h\text{-}A}$, cm^3/s	1.1×10^{-11}	1.1×10^{-11}	2.6×10^{-11}
w_e, s^{-1}	2.2×10^{-17}	2.6×10^{-17}	2.2×10^{-17}
w_h, s^{-1}	1.3×10^{-17}	1.3×10^{-17}	3.0×10^{-17}

The ionizing dose rate is taken equal to (a) the total absorbed dose and (b) the dose absorbed due to collisions including neutrons and gamma radiation (~80%) of total absorbed dose).

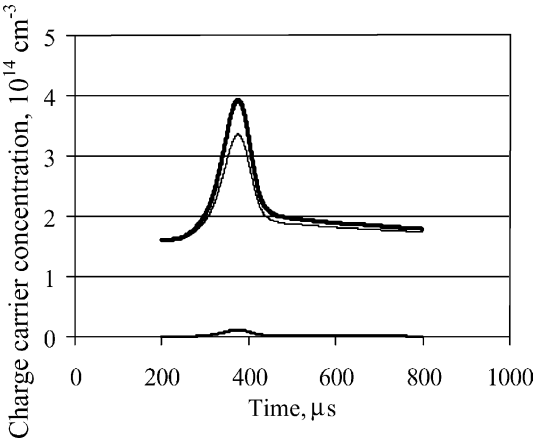

Fig. 2. Calculated time dependencies of the free hole concentration (line of the smallest thickness), free electron concentration (line of the intermediate thickness) and $f(t)$ function (line of the largest thickness).

The difference in the kinetic coefficients presented in Table 2 must be necessarily attributed to different efficiencies of RIC during reactor and proton irradiation. To compare the efficiencies of RIC during reactor and proton [8] irradiation, a dose rate dependence of the RIC in the steady-state was calculated for the case (a) of the reactor irradiation. Results of the calculation of the steady-state RIC under reactor irradiation are given in Fig. 3 together with the experimental values of the

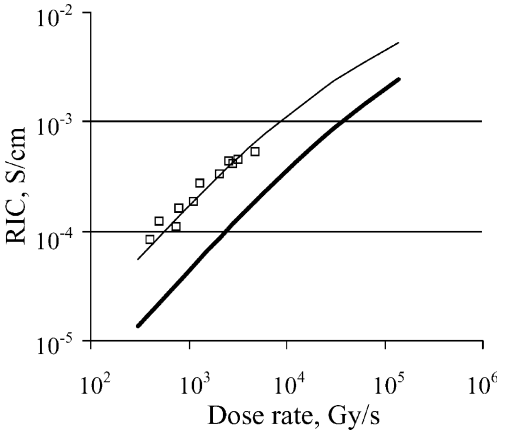

Fig. 3. Dependence of the steady-state RIC (S/cm) of 6H-SiC on the dose rate for proton irradiation (squares – experimental values, thin line – dependence obtained by fitting) and reactor irradiation (bold line – calculated dependence).

steady-state RIC under continuous proton irradiation [8] and a dose rate dependence obtained by fitting these experimental values (fitting parameters in Table 2 for proton irradiation). The dependence for reactor irradiation is shifted to the dose rates that four times higher as compared to the dependence of RIC during the proton irradiation.

During 17 MeV proton irradiation of SiC almost all the energy of irradiation (>99%) is converted to ionization. It seems obvious (see Fig. 3) that only 25% of the absorbed dose of reactor irradiation are responsible for the ionization, that is the part deposited by gamma irradiation. However, the ionizing losses during reactor irradiation are higher than 25% of the total absorbed dose, because the ionization is caused by both gamma irradiation and recoil atoms. In SiC, during elastic collisions of neutrons (fission spectrum) with Si and C nuclei, the mean energies of 80 and 170 keV/nucleus, respectively, are transferred. These collisions result in displacement of ions that spend major part (55% and 86%) of their energy to ionization. Therefore, during reactor irradiation of SiC, more than 65% of the deposited energy (considering gamma irradiation) is spent to electron–hole pair production. Moreover, in calculations of RIC using Eqs. (2)–(5), stronger deflection of the calculated time dependence of RIC from the dependence obtained experimentally during pulsed reactor irradiation was obtained for lower ionization losses.

5. Discussion

The apparent discrepancy between the steady-state dose rate dependencies of the RIC under proton and reactor irradiation can not be due to low ionizing losses only, but essentially non-uniform distribution of the ionizing losses in the bulk of the material during reactor irradiation. The electron–hole pair production and electron–hole recombination are not uniform. They are most intense in ion tracks and collision cascades, where sharp spikes of charge carrier production take place. However, this effect is not dominant, because of non-additive contributions to the electrical conductivity, that proportional to a mean charge carrier density.

To determine the effect of non-uniform distribution of ionizing losses on the mean charge carrier density, the Eq. (3) can be transformed into an equation for the increment of free electron density $\Delta n = n - n(0)$ and represented in a simplified shape

$$\frac{\mathrm{d}\Delta n}{\mathrm{d}t} = G(t) - w_{\mathrm{e-h}}\Delta n^2 - v\Delta n, \tag{9}$$

where v is the generalized coefficient of electron trapping. A similar equation can be written for holes. The steady-state solution of Eq. (9) is

$$\Delta n(G) = -\frac{v}{2w_{\mathrm{e-h}}} + \sqrt{\left(\frac{v}{2w_{\mathrm{e-h}}}\right)^2 + \frac{G}{w}}. \tag{10}$$

It is obvious that, in the case of random G, averaging the $\Delta n(G)$ gives the mean charge carrier density decreasing with increasing variance of G. During reactor irradiation the variance of G is larger than that during proton irradiation. Therefore, the RIC under reactor irradiation is lower than that under proton irradiation with the same dose rate.

The higher coefficient of electron–hole recombination obtained for reactor irradiation as compared to proton irradiation (Table 2) may be due to the intense electron–hole recombination in collision cascades. In fact, the coefficient of electron–hole recombination must be independent of the type of irradiation. It can be assumed that the right value of this coefficient is obtained for proton irradiation. However, an effective value is obtained for reactor irradiation, because uniform equations (Eqs. (2)–(5)) are used for a non-uniform problem.

The Eq. (10) with random G can be used to explain the low RIC of single crystal SiC under reactor irradiation. The simplest way is to assume intense charge carrier production with the rate G_{int} and, respectively, faster electron–hole recombination in microscopic regions occupying a small part $\delta V/V(< 10^{-3})$ of the bulk of SiC in the steady-state, whereas the charge carrier production rate in the rest of the bulk is approximately equal to zero. The rate G_{int} must be more than 10^3 times higher than the mean production rate. In these microscopic regions, the characteristic decay time for excess charge carriers (see Eq. (9)) is expressed by

$$\tau^{-1} = \sqrt{w_{\mathrm{e-h}}G_{\mathrm{int}}}, \tag{11}$$

that is equal to $\approx 10^{-8}$ s. The size l of the microscopic regions of intense charge carrier production and recombination is given by

$$l = \sqrt[3]{(F\sigma_{\mathrm{el}}N\tau)^{-1}\delta V/V}, \tag{12}$$

where F is the neutron flux ($<10^{17}$ n/cm^2 s), N is the atomic density of SiC (5×10^{22} atom/cm^3) the and σ_{el} is the elastic collision cross-sections ($\approx 10^{-24}$ cm^{-2}). The size l reaches 10^3 nm, which is in good agreement with the diffusion length of free electrons in ionic crystals (10^2–10^3 nm) [10].

In polycrystalline SiC, charge carrier trapping on grain boundaries is prevailing (see studies on BN [11]). Therefore, the regions of intense charge carrier production and recombination are confined within the grain if the grain size is smaller than the diffusion length of free electrons.

6. Conclusion

Lower RIC during reactor irradiation, as compared to proton, electron and gamma irradiation, is usually explained by the lower ionizing losses during reactor irradiation. In the present study, the magnitude of the RIC of single crystal SiC was compared by normalizing the ionizing dose rates. The RIC efficiency of the pulsed reactor irradiation was four times lower than that of proton irradiation. To explain the lower RIC efficiency, we point out the importance of cascade effects induced by pulsed neutrons, though the RIC consists of synergistic processes. The spatial distribution of the energy loss of pulsed neutrons is more irregular (local) than that of protons, due to the cascade production. The carrier production rate is not constant in the microscopic region of the material but abruptly changes by several orders of magnitude.

During the reactor irradiation, intense charge carrier production (at least 10^3 times faster) occurs in the microscopic regions (size up to $\sim$1000 nm) occupying a small part (lower than 10^{-3}) of the bulk SiC. The localized ionization is due to dense tracks of primary recoil ions and atomic collision cascades. Sharp spikes of charge carrier production may considerably contribute to the mean carrier-production rate, but, due to non-additive contributions, their effect on overall conductivity is not dominant.

The aspect of localized excitation is important also in practical SiC-materials irradiated by neutrons. The present estimate of the regions of intense charge carrier production is valid for single crystalline SiC and polycrystalline ones with the grain size larger than 1000 nm. In polycrystalline SiC with a grain size smaller than 1000 nm, the regions of intense charge carrier production are confined within the grain, where grain boundaries trap charge carriers. This process causes localized energy deposition in small grains (or in fibers of SiC composites) and may alter the kinetics and the characters of structural and phase transformation.

References

[1] P. Fenici, A.J. Frias Rebelo, R.H. Jones, A. Kohyama, L.L. Snead, JNM 258–263 (1998) 215.
[2] A.A. Lebedev, Semiconductors 33 (1999) 129.
[3] D.A. Evans, in: P.T. Lamdsberg (Ed.), Solid State Theory – Methods and Applications, John Wiley, New York, 1969, p. 287.
[4] V.A.J. van Lint, T.M. Flanagan, R.E. Leadon, J.A. Naber, V.G. Rogers, Mechanisms of Radiation Effects in Electronic Materials, vol. 1, John Wiley, New York, 1980.
[5] S. Kasahara, Y. Katano, S. Shimanuki, K. Nakata, H. Ohno, JNM 191–194 (1992) 579.
[6] K. Nakata, S. Shimanuki, Y. Katano, H. Ohno, H. Katsuta, JNM 155–157 (1988) 307.
[7] P.V. Demenkov, O.A. Plaksin, V.A. Stepanov, P.A. Stepanov, V.M. Chernov, Tech. Phys. Lett. 26 (2000) 57.
[8] H. Amekura, N. Kishimoto, K. Kono, Mater. Sci. Forum 338–342 (2000) 977.
[9] MCNP – a General Monte Carlo Code for Neutron and Photon Transport, J.F. Briesmeister (Ed.), LANL LA-7396, Rev. 2 1986.
[10] M.A. Elango, Elementary Inelastic Radiation-Induced Processes, Nauka, Moscow, 1988.
[11] B.K. Kardashev, P.V. Demenkov, O.A. Plaksin, V.A. Stepanov, P.A. Stepanov, V.M. Chernov, Phys. Solid State 43 (2001) 2087.